Quantum Limits of Covert Target Detection

Guo Yao Tham [1,*] Ranjith Nair [1,†] and Mile Gu [1,2,3,‡]

[1]*Nanyang Quantum Hub, School of Physical and Mathematical Sciences, Nanyang Technological University, 21 Nanyang Link, Singapore 637371*
[2]*Centre for Quantum Technologies, National University of Singapore, 3 Science Drive 2, Singapore 117543*
[3]*MajuLab, CNRS-UNS-NUS-NTU International Joint Research Unit, UMI 3654, 117543 Singapore*

In covert target detection, Alice attempts to send optical or microwave probes to determine the presence or absence of a weakly reflecting target embedded in thermal background radiation within a target region, while striving to remain undetected by an adversary, Willie, who is co-located with the target and collects all light that does not return to Alice. We formulate this problem in a realistic setting and derive quantum-mechanical limits on Alice's error probability performance in entanglement-assisted target detection for any fixed level of her detectability by Willie. We demonstrate how Alice can approach this performance limit using two-mode squeezed vacuum probes in the regime of small to moderate background brightness, and how such protocols can outperform any conventional approach using Gaussian-distributed coherent states. In addition, we derive a universal performance bound for nonadversarial quantum illumination without requiring the passive-signature assumption.

Alice wishes to interrogate a distant region embedded in a thermal background for the presence or absence of a target adversary by probing it with a microwave or optical beam and monitoring the resulting reflections. Meanwhile, the adversary, Willie, monitors his thermal background for statistical deviations from thermal noise, aiming to detect if Alice is actively probing him. In this cat-and-mouse game, how can Alice maximize her probability of correctly detecting Willie while minimizing Willie's chances of knowing he is being probed? This question falls under the domain of *covert sensing* and naturally arises in the adversarial arms race between radar and radar detectors [1].

Alice faces a trade-off between performance and covertness. Sending a probe with greater energy relative to the background can better sense Willie but also risks being detected. A better idea would be to prepare coherent state probes $\{|\alpha\rangle\}$ with field amplitude α Gaussianly distributed in phase space around the origin to perfectly mimic the statistics of the thermal background, which allows some chance of detecting Willie while being perfectly covert. However, what is the ultimate limit of Alice's performance, and would moving toward this limit be facilitated by employing nonclassical light, as is well-known for quantum illumination (henceforth abbreviated as QI) in nonadversarial settings [2–9]? Indeed, several other covert protocols

have been introduced in the quantum continuous-variable setting [10–15].

To answer our question, we suppose that Alice wishes to remain ϵ-covert, i.e., that the probability of Willie detecting her is at most $1/2 + \epsilon$. We then ask: What is Alice's minimal error probability for detecting Willie? We obtain a closed-form lower bound on this error probability as a function of ϵ, the number of available optical modes M, and levels of loss and noise in the system. We show that two-mode squeezed vacuum (TMSV) probes can approach this limit in certain regimes. Comparing TMSV performance with that of the aforementioned Gaussian-distributed coherent state (GCS) probes, our results show that TMSV probes enable a reduction in error probability that scales exponentially with M.

To ensure our bounds apply to all adversaries, we assume Willie can detect any statistical deviation from the thermal background noise—including those resulting from using multimode vacuum probes. This involves dropping the commonly adopted "no passive signature" (NPS) assumption in quantum illumination [2–9], a mathematically expedient but nonphysical approximation whereby the background temperature depends in a fine-tuned manner on whether the target is present or absent so as to ensure Alice cannot detect Willie using a vacuum probe. The new techniques we develop for this more mathematically complex setting have immediate relevance to general QI, supporting recent interest in dropping the NPS assumption therein [16–19]. Indeed, our Letter provides as a natural byproduct the first universal performance limit for QI without the NPS approximation.

---

*Contact author: tham0157@e.ntu.edu.sg
†Contact author: ranjith.nair@ntu.edu.sg
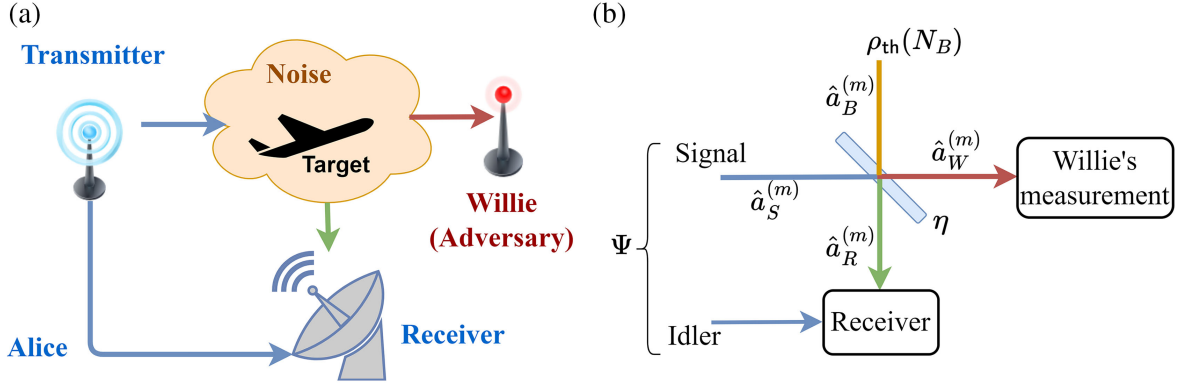‡Contact author: gumile@ntu.edu.sg

FIG. 1. (a) In covert target detection, Alice (A) attempts to detect the presence of the adversary Willie (W) using an ancilla-entangled probe while remaining undetected herself. In the beam splitter model (b), Alice prepares a joint state Ψ with M signal (S) and idler modes (I). Each signal mode $\hat{a}_S^{(m)}$ is either replaced by a background mode $\hat{a}_B^{(m)}$ when Willie is absent, or mixed with the background at a beam splitter with reflectance $\eta \ll 1$ representing the target. Alice makes an optimal measurement on the return modes $\{\hat{a}_R^{(m)}\}_{m=1}^M$ along with the idler system. Willie, when present, makes an optimal measurement on all his modes $\{\hat{a}_W^{(m)}\}_{m=1}^M$.

Problem setup—Target detection is illustrated in Fig. 1. Alice (A) wishes to detect the absence ($h = 0$) or presence ($h = 1$) of a weakly reflecting target (the two cases being assumed to be equally likely for simplicity) with reflectance $\eta \ll 1$ [20]. The target is immersed in a thermal background such that each background mode is in a thermal state $\rho_{\text{th}}(N_B) = \sum_{n=0}^{\infty} N_B^n/(N_B + 1)^{n+1}|n\rangle\langle n|$ with average photon number N_B. Alice controls both the transmitter and receiver [21], and can prepare M signal modes. Thus, any covert sensing protocol involves preparing some incident probe state

$$|\psi\rangle_{IS} = \sum_{\mathbf{n}} \sqrt{p_{\mathbf{n}}}|\chi_{\mathbf{n}}\rangle_I|\mathbf{n}\rangle_S, \qquad (1)$$

where $|\mathbf{n}\rangle_S = |n_1\rangle_1|n_2\rangle_2 \cdots |n_M\rangle_M$ is an M-mode number state of the *signal* (S) system, $\{|\chi_{\mathbf{n}}\rangle_I\}$ are normalized (not necessarily orthogonal) states of an *idler* (I) system, and $p_{\mathbf{n}}$ is the probability mass function (PMF) of $\mathbf{n}$. The signal modes are sent to probe the target region while the idler is held losslessly. In the return (R) modes, Alice obtains an h-dependent return-idler state $\rho_{IR}^{(h)}$ that she measures to make a guess h_{est} for the value of h. Alice's performance is given by the *error probability* P_e^A, i.e., the probability that $h_{\text{est}} \neq h$.

The adversary, Willie (W), is situated at the target's location. He is constrained only by the laws of physics and can have prior knowledge of which probe $\Psi = |\psi\rangle\langle\psi|_{IS}$ Alice plans to use. Thus any statistical deviation of the state intercepted by Willie from the M-mode thermal background $\rho_{\text{th}}(N_B)^{\otimes M}$ allows him to achieve an error probability P_e^W that is better than guessing randomly (this assumes Willie's prior of being probed is uniform. We discuss the case of unequal prior probabilities for Willie in Sec. III.A of the Supplemental Material [22]). Alice's probe state is said to be ϵ-covert if

$$P_e^W \geq 1/2 - \epsilon. \qquad (2)$$

We then ask: What is Alice's minimal error probability P_e^A (as a function of M) when optimized over ϵ-covert probes?

We model the weakly reflecting object by a beam splitter with reflectance $\eta \ll 1$ [20]. Let $\hat{a}_S^{(m)}$ and $\hat{a}_B^{(m)}$ be annihilation operators of the corresponding signal and background modes (see Fig. 1). Then

$$\hat{a}_R^{(m)} = \sqrt{\eta^{(h)}}\hat{a}_S^{(m)} + \sqrt{1 - \eta^{(h)}}\hat{a}_B^{(m)} \qquad (3)$$

represents the annihilation operator of the mth mode returning to Alice, where $\eta^{(0)} = 0$ and $\eta^{(1)} = \eta$. When Willie is present ($h = 1$), he receives the modes $\hat{a}_W^{(m)}$ for each $m = 1, \ldots, M$ from the other output of the beam splitter so that

$$\hat{a}_W^{(m)} = \sqrt{1 - \eta}\hat{a}_S^{(m)} - \sqrt{\eta}\hat{a}_B^{(m)}. \qquad (4)$$

Thus Alice faces the hypothesis test

$$\begin{aligned}
\text{H}_0 &: \rho_0 = (\text{Tr}_S \Psi) \otimes \rho_{\text{th}}(N_B)^{\otimes M}, \\
\text{H}_1 &: \rho_1 = \left(\text{id}_I \otimes \mathcal{L}_{\eta,N_B}^{\otimes M}\right)\Psi,
\end{aligned} \qquad (5)$$

where $\mathcal{L}_{\kappa,N}$ denotes a thermal loss (or noisy attenuator) channel of transmittance κ and excess noise N [28]. Meanwhile, Willie faces his own hypothesis test

$$\begin{aligned}
\text{H}_0' &: \sigma_0 = \rho_{\text{th}}(N_B)^{\otimes M}, \\
\text{H}_1' &: \sigma_1 = \mathcal{L}_{1-\eta,N_B}^{\otimes M}(\text{Tr}_I \Psi).
\end{aligned} \qquad (6)$$

to decide whether Alice has sent a probe (H_1') or not (H_0').

Assuming that both parties make optimal quantum measurements and that their hypotheses are equally likely, their resulting average error probabilities are given by the Helstrom formula [29]:

$$P_e^A = 1/2 - \|\rho_0 - \rho_1\|_1/4 \leq \inf_{0 \leq s \leq 1} \operatorname{Tr} \rho_0^s \rho_1^{1-s}/2, \quad (7)$$

$$P_e^W = 1/2 - \|\sigma_0 - \sigma_1\|_1/4 \leq \inf_{0 \leq s \leq 1} \operatorname{Tr} \sigma_0^s \sigma_1^{1-s}/2, \quad (8)$$

where $\|X\|_1 := \operatorname{Tr}\sqrt{X^\dagger X}$ is the trace norm. We have also indicated the *quantum Chernoff bound* [30] that is an exponentially tight upper bound on the average error probability.

The above framework deviates in several significant ways from previous studies of covert target detection [31]. Firstly, our notion of ϵ-covertness defined by way of Willie's error probability has clear operational significance. Previous formulations use relative entropy [31], which provides no upper bound on the error probability [32] and cannot therefore be used to derive a performance limit in our setting. Secondly, our framework fixes the background brightness at N_B regardless of whether a target is present or absent. In contrast, prior work makes the NPS assumption which fine-tunes background brightness from its nominal value of N_B to $N_B/(1-\eta)$ when the target is present [33]. Under this assumption, Willie's null hypothesis is to receive multimode vacuum states from Alice [31]. In our setting, Willie, being bathed in thermal radiation from all directions, receives a thermal state with the same brightness as the background when Alice is absent. Thus, Willie's null hypothesis is based on multimode probes that are statistically identical to the thermal background.

Dropping the NPS assumption induces new qualitative behavior in both nonadversarial and covert QI. Alice's performance then explicitly depends on the number M of signal modes, e.g., the available time-bandwidth product for temporal modes. This is in line with findings for other quantum sensing and discrimination problems for which the mode number is an important resource aiding the performance even when vacuum probes are used [34–37]. For ϵ-covert illumination, we can quantify the performance of a target detection protocol by defining its Chernoff exponent $\chi := -\lim_{M \to \infty}(1/M) \ln P_e^A$. A difference Δ in the exponents of two probes implies a ratio of $e^{-\Delta M}$ between their error probabilities P_e^A, which scales exponentially in M.

Illumination with passive signature—We first derive analytical bounds on Alice's performance in the non-adversarial setting, i.e., for standard QI but without the NPS approximation. In Sec. II of the Supplemental Material, we show a more general result: For $b \in \{0, 1\}$, let states $\rho_b := (\mathrm{id}_I \otimes \mathcal{L}_{\kappa_b,N_b}^{\otimes M})\Psi$ be the respective output states of any two thermal loss channels $\mathcal{L}_{\kappa_0,N_0}$ and $\mathcal{L}_{\kappa_1,N_1}$ in

response to the input Ψ of Eq. (1). Then the output fidelity $F := \operatorname{Tr}\sqrt{\sqrt{\rho_0}\rho_1\sqrt{\rho_0}}$ satisfies

$$F \geq \nu^M \sum_{n=0}^{\infty} p_n \left[\nu\sqrt{\tilde{\kappa}_0\tilde{\kappa}_1} + \sqrt{(1-\tilde{\kappa}_0)(1-\tilde{\kappa}_1)} \right]^n, \quad (9)$$

where $\nu = (\sqrt{G_0 G_1} - \sqrt{(G_0-1)(G_1-1)})^{-1}$ and $\tilde{\kappa}_b = \kappa_b/G_b$ for $G_b = (1-\kappa_b)N_b + 1$. For target detection, we set $\kappa_0 = 0$, $\kappa_1 = \eta$, $N_0 = N_1 = N_B$ and use the Fuchs-van de Graaf inequality [38] to conclude that

$$P_e^A \geq \frac{1}{2}\left[1 - \sqrt{1 - \nu^{2M}\left[\sum_{n=0}^{\infty} p_n(1 - \gamma_{\eta,N_B})^{\frac{n}{2}} \right]^2} \right]$$

$$\geq \frac{1}{2}\left[1 - \sqrt{1 - \nu^{2M}(1 - \gamma_{\eta,N_B})^{\mathcal{N}_S}} \right], \quad (10)$$

where $\gamma_{\eta,N_B} = \{\eta/[(1-\eta)N_B + 1]\}$, $\mathcal{N}_S := \sum_{n=0}^{\infty} np_n$ is the total signal energy, and we have used Jensen's inequality in the last step. The above result gives the ultimate limit of Alice's performance in QI with the passive signature assumption. It contrasts with the ultimate quantum limits of NPS QI derived in Ref. [39] [see Eqs. (12)–(13) therein], which do not include the M-dependent factor ν^{2M} characteristic of the passive signature.

Necessary condition for ϵ-covertness—To incorporate the covertness constraint, we formulate a necessary condition for ϵ-covertness. Suppose that Alice transmits the probe Ψ of Eq. (1) with signal energy $\mathcal{N}_S$. The Fuchs-van de Graaf inequality $P_e^W \leq F(\sigma_0, \sigma_1)/2$ that relates the trace distance to the fidelity [38] between Willie's hypothesis states (6) implies that $F(\sigma_0, \sigma_1) \geq 1-2\epsilon$ is a necessary condition for ϵ-covertness. In Ref. [22], Sec. III, we use this to show that

$$\sum_{n=0}^{\infty} \sqrt{q_n} \sqrt{\binom{n+M-1}{n} \frac{N_B^n}{(N_B+1)^{n+M}}} \geq 1 - 2\epsilon \quad (11)$$

is a necessary condition for ϵ-covertness, where $q_{\mathbf{n}} = \langle \mathbf{n}|\sigma_1|\mathbf{n}\rangle_W$ and $\{q_n = \sum_{\mathbf{n}:n_1+\cdots+n_M} q_{\mathbf{n}}\}_{n=0}^{\infty}$ is the PMF of the total photon number seen by Willie under H_1'.

Signal energy constraints—The above condition then implies bounds on the allowed signal energies. Clearly, for $\epsilon = 0$, an M-mode quantum or classical probe with perfect covertness must have signal energy $\mathcal{N}_S = MN_B$ to match perfectly with Willie's thermal background. For $\epsilon > 0$, we use Lagrange multipliers to extremize the average energy $\sum_{n=0}^{\infty} nq_n$ of σ_1 under the constraint of Eq. (11), which then constrains the probe energy $\mathcal{N}_S = [\sum_{n=0} nq_n - \eta N_B]/(1-\eta)$ [cf. Eq. (4)]. We find (Fig. 2) that the probe energy must lie in a bounded region around MN_B that gets smaller as ϵ is reduced—see Ref. [22], Sec. IV, for details. Curve fitting indicates that the per-mode probe energy $N_S := \mathcal{N}_S/M$ varies between
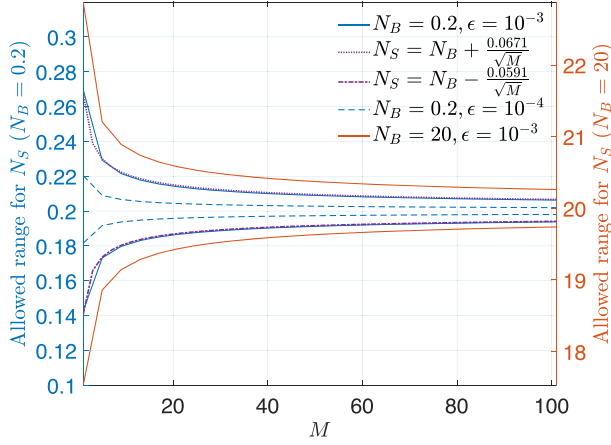
FIG. 2. The maximum and minimum allowed per-mode energy N_S for an ϵ-covert probe according to Eq. (11) as a function of M with $N_B = 0.2$ and $\epsilon = 10^{-3}$ (solid blue) and $\epsilon = 10^{-4}$ (dashed blue). Curve fitting produced the estimates $N_B + 0.0671/\sqrt{M}$ and $N_B - 0.0591/\sqrt{M}$ for the maximum and minimum energy curves for $\epsilon = 10^{-3}$. The allowed range of N_S for $N_B = 20$, $\epsilon = 10^{-3}$ is also shown (red). $\eta = 0.01$ for all curves.

$\sim N_B \pm A_\pm/\sqrt{M}$, where A_+ and A_- depend only on η, N_B, and ϵ (see Fig. 2). To maintain covertness, Alice's per-mode probe must look progressively more similar to the thermal background as we increase M. In a significant departure from standard QI, it no longer makes operational sense to consider the scaling of Alice's performance with signal energy $\mathcal{N}_S$. Instead, the key resource is the number of available optical modes M.

Fundamental limits under ϵ-covertness—The thermal loss channel $\mathcal{L}_{1-\eta,N_B}$ connecting the modes in S to those in W [cf. Eq. (6)] admits the decomposition

$$\mathcal{L}_{1-\eta,N_B} = \mathcal{A}_G \circ \mathcal{L}_{(1-\eta)/G} \qquad (12)$$

into a quantum-limited amplifier $\mathcal{A}_G$ of gain $G = \eta N_B + 1$ and a pure-loss channel $\mathcal{L}_{(1-\eta)/G}$ of transmittance $(1-\eta)/G$ [40]. The right-hand side of the bound of Eq. (10) is expressed in terms of the *probability generating function* (PGF) $\mathcal{P}_S(\xi)$ of the total photon number in S, defined as $\mathcal{P}_S(\xi) := \sum_{n=0}^{\infty} p_n \xi^n$ evaluated at $\xi = \sqrt{1 - \gamma_{\eta,N_B}}$. Haus has developed relations connecting the input and output photon number PGFs of these single-mode quantum-limited channels [41]. In Ref. [22], Sec. V, we use the decomposition (12) to extend these to multimode thermal loss channels and find the one-to-one mapping between the photon number PGF of the probe and the PGF $\mathcal{P}_W(\xi) := \sum_{n=0}^{\infty} q_n \xi^n$ of the total photon number in Willie's modes under H_1'. By connecting $\mathcal{P}_W(\xi)$ to the covertness condition of Eq. (11), we show in Ref. [22], Sec. VI, that

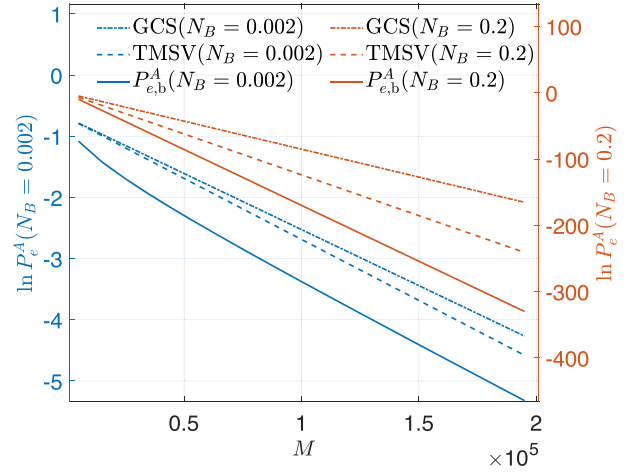$$P_e^A \geq \frac{1 - \sqrt{1 - (1-2\epsilon)^4 f_{\eta,N_B}^{2M}}}{2}, \qquad (13)$$

FIG. 3. The lower bound Eq. (13) (solid) on Alice's error probability is compared to that of ϵ-covert TMSV (dashed) and GCS probes (dash-dotted line) for $N_B = 0.2$ (blue) and $N_B = 0.002$ (red). $\epsilon = 10^{-3}$ for both. For large M, the ratio of the error exponents predicted by the bound (13) and of TMSV probes are 1.37 (for $N_B = 0.2$) and 1.16 (for $N_B = 0.002$) respectively.

where $f_{\eta,N_B} = \nu[N_B + 1 - (N_B/x)][\eta N_B(1-x) + 1]$, $x = 1 - \{\Theta/\eta[1 + N_B(1-\Theta)]\}$ and $\Theta = [\sqrt{(1-\eta)(N_B+1)}/\sqrt{1 + (1-\eta)N_B}]$. While this equation looks complex, it provides a universal, analytical and probe-independent lower bound for Alice's error probability for any desired covertness level ϵ.

Figure 3 compares the lower bound of Eq. (13) to quantum TMSV and classical GCS probes. For each M, we consider the M-mode an independently and identically distributed (IID) TMSV state with per-mode signal energy N_S chosen to be the maximum allowable by the covertness constraint (see Ref. [22], Sec. VI.C for details). When limited to classical probes, Alice can generate GCS probes—coherent states in each signal mode with amplitude $\alpha \in \mathbb{C}$ chosen according to a product circular Gaussian distribution $P(\alpha) = [1/(\pi N_S)]e^{-|\alpha|^2/N_S}$ with per-mode energy identical to the TMSV probe (In this case, Alice's measurement can be informed by knowledge of the amplitude transmitted in each of the M shots). For $N_B = 0.2$, the large-M error exponent achieved by TMSV probes was about a factor of 1.37 lower than that of the bound, with the discrepancy becoming smaller for smaller N_B, along with the gap between the GCS and TMSV exponents.

Perfect covertness—Consider the special case of perfect covertness, i.e., $\epsilon = 0$. Among quantum probes, the M-mode TMSV state with signal brightness $N_S = N_B$ is the only viable pure state (modulo unitary transformations on the idler) quantum probe. Among classical probes, only the IID GCS probes with $N_S = N_B$ are possible. To compare their target detection performance, we calculate the quantum Chernoff exponents χ (Ref. [22], Sec. I).
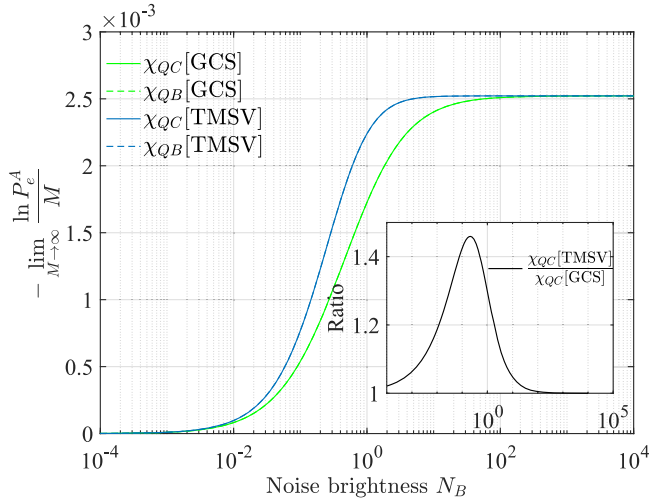
FIG. 4. The quantum Chernoff (QC) (solid) and (closely overlapping) quantum Bhattacharyya (QB) (dashed) error probability exponents as a function of the noise brightness N_B with $\eta = 0.01$ for perfectly covert TMSV (blue) and GCS (green) probes. The inset shows the ratio of the exponents for the TMSV and GCS probes, which is maximized for $N_B \simeq 0.2$.

These are very close to the quantum Bhattacharyya ($s = 1/2$) exponents, which have the approximate forms

$$\chi_{\mathrm{TMSV}} \simeq \ln\left[1 - \frac{\eta}{4}\left(1 - \frac{1}{(2N_B+1)^2}\right)\right],$$

$$\chi_{\mathrm{GCS}} \simeq \ln\left[1 - 2\eta N_B\left(N_B - \sqrt{N_B(N_B+1)} + \frac{1}{2}\right)\right]. \quad (14)$$

The results are compared in Fig. 4. When N_B is small, the requirement $N_S \ll 1$ for quantum advantage in target detection (similar to NPS QI [2,39]) aligns with covertness requirements ($N_S \simeq N_B$). However, this advantage is small since GCS probes of the same N_S have identical covertness and near-identical detection performance. When $N_B \gg 1$, requirements for optimal detection advantage ($N_S \ll 1$) conflict with that of covertness ($N_S \approx N_B$). Thus, we anticipate the maximum advantage at some intermediate value of N_B. This turns out to be $N_B \sim 0.2$ with a maximum ratio of $\simeq 1.45$. For $N_B = 0.575$ and $M = 10^6$ (current technology already reaches $M \sim 10^6$ [5]), TMSV probes offer a $\sim 10^{237}$-fold reduction in error probability.

Discussion—We introduced an operational framework for covert quantum target detection: Alice wishes to minimize her error probability in detecting an adversary Willie in thermal noise, subject to an ϵ-covertness constraint and assuming Willie can detect any deviation from the thermal background. Our lower bound (13) is a fundamental limit on an ϵ-covert Alice's performance. As indicated in Fig. 3, the lower bound can be approximately achieved using a TMSV in the optical regime of $N_B \ll 1$, with the maximum advantage over the Gaussian-distributed coherent states being obtained for $N_B \simeq 0.2$. The

achievable quantum advantage—measured by the factor by which entangled probes can reduce error probabilities—scales exponentially with the number of optimal modes M.

There are multiple directions for continuation. Our choice of TMSV probes was motivated by their experimental accessibility and demonstrated near optimality for $N_B \ll 1$. Are they also near-optimal for general N_B? (cf. numerical studies for standard QI [42]). Meanwhile, the optimality of the GCS scheme among all classical methods remains a conjecture for general ϵ-covertness (it is clearly true for $\epsilon = 0$). Toward practical realization, we will also need to understand how such quantum advantage can be accessed using linear-optics-based measurements, mirroring similar studies in standard QI [43]). Meanwhile, scenarios where Willie has further practical constraints (e.g., he cannot collect all the modes that do not return to Alice after reflection at the target), will be of great relevance in more downstream use cases. Beyond covert sensing, the regime of validity of the no passive signature approximation is a topic of ongoing study in nonadversarial target detection [16–19], where our analytical bound (10) will certainly be relevant.

Beyond target detection, suitable modification of Willie's hypothesis test and Alice's performance metric could enable applying our techniques to other sensing problems where passive signature is present. In particular, our fidelity-based approach encompasses all ϵ-covert probes without further assumptions on, e.g., their photon number variance [13,14], and may yield explicit M-dependent performance bounds for protocols such as covert phase and transmittance sensing [13–15]. Finally, our fidelity bounds of Eqs. (9) on the outputs of thermal loss channels should be useful for obtaining fundamental performance bounds for schemes such as quantum reading [44], pattern recognition [45], and channel position finding [46,47].

[1] P. E. Pace, *Detecting and Classifying Low Probability of Intercept Radar* (Artech House, Norwood, 2004), Vol. 1.

[2] S.-H. Tan, B. I. Erkmen, V. Giovannetti, S. Guha, S. Lloyd, L. Maccone, S. Pirandola, and J. H. Shapiro, Quantum

illumination with Gaussian states, Phys. Rev. Lett. **101,** 253601 (2008).

[3] S. Pirandola, B. R. Bardhan, T. Gehring, C. Weedbrook, and S. Lloyd, Advances in photonic quantum sensing, Nat. Photonics **12,** 724 (2018).

[4] E. Polino, M. Valeri, N. Spagnolo, and F. Sciarrino, Photonic quantum metrology, AVS Quantum Sci. **2,** 024703 (2020).

[5] J. H. Shapiro, The quantum illumination story, IEEE Aerospace Electron. Syst. Mag. **35,** 8 (2020).

[6] R. G. Torromé, N. B. Bekhti-Winkel, and P. Knott, Introduction to quantum radar, arXiv:2006.14238.

[7] G. Sorelli, N. Treps, F. Grosshans, and F. Boust, Detecting a target with quantum entanglement, IEEE Aerospace Electron. Syst. Mag. **37,** 68 (2022).

[8] A. Karsa, A. Fletcher, G. Spedalieri, and S. Pirandola, Quantum illumination and quantum radar: A brief overview, Rep. Prog. Phys. **87,** 094001 (2024).

[9] R. Gallego Torromé and S. Barzanjeh, Advances in quantum radar and quantum LiDAR, Prog. Quantum Electron. **93,** 100497 (2024).

[10] B. A. Bash, A. H. Gheorghe, M. Patel, J. L. Habif, D. Goeckel, D. Towsley, and S. Guha, Quantum-secure covert communication on bosonic channels, Nat. Commun. **6,** 1 (2015).

[11] M. S. Bullock, C. N. Gagatsos, S. Guha, and B. A. Bash, Fundamental limits of quantum-secure covert communication over bosonic channels, IEEE J. Sel. Areas Commun. **38,** 1 (2020).

[12] R. Di Candia, H. Yiğitler, G. S. Paraoanu, and R. Jäntti, Two-way covert quantum communication in the microwave regime, PRX Quantum **2,** 020316 (2021).

[13] B. A. Bash, C. N. Gagatsos, A. Datta, and S. Guha, Fundamental limits of quantum-secure covert optical sensing, in *2017 IEEE International Symposium on Information Theory (ISIT)* (IEEE, Piscataway, 2017), pp. 3210–3214.

[14] C. N. Gagatsos, B. A. Bash, A. Datta, Z. Zhang, and S. Guha, Covert sensing using floodlight illumination, Phys. Rev. A **99,** 062321 (2019).

[15] S. Hao, H. Shi, C. N. Gagatsos, M. Mishra, B. Bash, I. Djordjevic, S. Guha, Q. Zhuang, and Z. Zhang, Demonstration of entanglement-enhanced covert sensing, Phys. Rev. Lett. **129,** 010501 (2022).

[16] Y. Jo, S. Lee, Y. S. Ihn, Z. Kim, and S.-Y. Lee, Quantum illumination receiver using double homodyne detection, Phys. Rev. Res. **3,** 013006 (2021).

[17] S.-Y. Lee, Y. Jo, T. Jeong, J. Kim, D. H. Kim, D. Kim, D. Y. Kim, Y. S. Ihn, and Z. Kim, Observable bound for Gaussian illumination, Phys. Rev. A **105,** 042412 (2022).

[18] K. M. Shafi, A. Padhye, and C. M. Chandrashekar, Quantum illumination using polarization-path entangled single photons for low reflectivity object detection in a noisy background, Opt. Express **31,** 32093 (2023).

[19] T. Volkoff, Not even 6 dB: Gaussian quantum illumination in thermal background, J. Phys. A: Math. Theor. **57,** 065301 (2024).

[20] η represents the residual reflectivity in the entire trip from transmitter to receiver and thus includes diffraction losses as well as the reflectivity of the target object itself.

[21] If the radar configuration is bistatic, we assume that the idler modes can be transported losslessly to the receiver's location.

[22] See Supplemental Material at http://link.aps.org/supplemental/10.1103/PhysRevLett.133.110801 for detailed derivations of the results presented in the paper, which additionally cites Refs. [23–27].

[23] L. Banchi, S. L. Braunstein, and S. Pirandola, Quantum fidelity for arbitrary Gaussian states, Phys. Rev. Lett. **115,** 260501 (2015).

[24] K. Sharma, M. M. Wilde, S. Adhikari, and M. Takeoka, Bounding the energy-constrained quantum and private capacities of phase-insensitive bosonic Gaussian channels, New J. Phys. **20,** 063025 (2018).

[25] R. Nair, Quantum-limited loss sensing: Multiparameter estimation and Bures distance between loss channels, Phys. Rev. Lett. **121,** 230801 (2018).

[26] M. A. Nielsen and I. L. Chuang, *Quantum Computation and Quantum Information* (Cambridge University Press, Cambridge, England, 2000).

[27] R. Nair, Discriminating quantum-optical beam-splitter channels with number-diagonal signal states: Applications to quantum reading and target detection, Phys. Rev. A **84,** 032312 (2011).

[28] A. Serafini, *Quantum Continuous Variables: A Primer of Theoretical Methods* (CRC Press, 2017).

[29] C. W. Helstrom, *Quantum Detection and Estimation Theory* (Academic Press, New York, 1976).

[30] K. M. R. Audenaert, J. Calsamiglia, R. Muñoz-Tapia, E. Bagan, L. Masanes, A. Acín, and F. Verstraete, Discriminating states: The quantum Chernoff bound, Phys. Rev. Lett. **98,** 160501 (2007).

[31] M. Tahmasbi, B. A. Bash, S. Guha, and M. Bloch, Signaling for covert quantum sensing, in *2021 IEEE International Symposium on Information Theory (ISIT)* (2021), pp. 1041–1045.

[32] K. M. R. Audenaert, Comparisons between quantum state distinguishability measures, Quantum Inf. Comput. **14,** 31 (2014).

[33] Specifically, under the NPS assumption, the channel between S and R is taken to be $\mathcal{L}_{\eta,N_B/(1-\eta)}$ in each mode and that between S and W is $\mathcal{L}_{1-\eta,N_B/(1-\eta)}$ in each mode when Willie is present, while σ_0 is taken to be $\mathcal{L}_{1-\eta,N_B/(1-\eta)}^{\otimes M}(|0\rangle\langle 0|_S^{\otimes M}) = \rho_{\text{th}}(\eta N_B/(1-\eta))^{\otimes M}$.

[34] R. Nair, G. Y. Tham, and M. Gu, Optimal gain sensing of quantum-limited phase-insensitive amplifiers, Phys. Rev. Lett. **128,** 180506 (2022).

[35] R. Jönsson and R. Di Candia, Gaussian quantum estimation of the loss parameter in a thermal environment, J. Phys. A **55,** 385301 (2022).

[36] H. Shi and Q. Zhuang, Ultimate precision limit of noise sensing and dark matter search, npj Quantum Inf. **9,** 27 (2023).

[37] R. Nair and M. Gu, Quantum sensing of phase-covariant optical channels, arXiv:2306.15256.

[38] C. Fuchs and J. van de Graaf, Cryptographic distinguishability measures for quantum-mechanical states, IEEE Trans. Inf. Theory **45,** 1216 (1999).

[39] R. Nair and M. Gu, Fundamental limits of quantum illumination, Optica **7,** 771 (2020).

[40] F. Caruso, V. Giovannetti, and A. S. Holevo, One-mode bosonic Gaussian channels: A full weak-degradability classification, New J. Phys. **8,** 310 (2006).

[41] H. A. Haus, *Electromagnetic Noise and Quantum Optical Measurements* (Springer Science & Business Media, New York, 2000).

[42] M. Bradshaw, L. O. Conlon, S. Tserkis, M. Gu, P. K. Lam, and S. M. Assad, Optimal probes for continuous-variable quantum illumination, Phys. Rev. A **103**, 062413 (2021).

[43] H. Shi, B. Zhang, J. H. Shapiro, Z. Zhang, and Q. Zhuang, Optimal entanglement-assisted electromagnetic sensing and communication in the presence of noise, Phys. Rev. Appl. **21**, 034004 (2024).

[44] S. Pirandola, Quantum reading of a classical digital memory, Phys. Rev. Lett. **106**, 090504 (2011).

[45] L. Banchi, Q. Zhuang, and S. Pirandola, Quantum-enhanced barcode decoding and pattern recognition, Phys. Rev. Appl. **14**, 064026 (2020).

[46] Q. Zhuang and S. Pirandola, Entanglement-enhanced testing of multiple quantum hypotheses, Commun. Phys. **3**, 103 (2020).

[47] J. L. Pereira, L. Banchi, Q. Zhuang, and S. Pirandola, Idler-free channel position finding, Phys. Rev. A **103**, 042614 (2021).